

A. LI  
S.C. LIU  
K.W. SU  
Y.L. LIAO  
S.C. HUANG  
Y.F. CHEN<sup>✉</sup>  
K.F. HUANG

# InGaAsP quantum-wells saturable absorber for diode-pumped passively *Q*-switched 1.3- $\mu\text{m}$ lasers

Department of Electrophysics, National Chiao Tung University, 1001 TA Hsueh Road, Hsinchu, 30050 Taiwan

Received: 15 January 2006/Revised version: 24 March 2006  
Published online: 20 May 2006 • © Springer-Verlag 2006

**ABSTRACT** We demonstrate the first use of InGaAsP quantum wells as a saturable absorber in the *Q*-switching of a diode-pumped Nd-doped 1.3  $\mu\text{m}$  laser. The barrier layers of the InGaAsP quantum-well device are designed to be a strong absorber for the suppression of the transition channel at 1.06  $\mu\text{m}$ . With an incident pump power of 1.8 W, an average output power of 160 mW with a *Q*-switched pulse width of 19 ns at a pulse repetition rate of 38 kHz was obtained.

**PACS** 42.60.Gd; 42.55.Xi; 42.65.Re

## 1 Introduction

Compact, rugged, all-solid-state *Q*-switched lasers at 1.3  $\mu\text{m}$  wavelength are of practical importance for numerous applications such as medical diagnostics, fiber sensing, distance measurements, intracavity optical parametric oscillators, and intracavity Raman conversion. Compared with active *Q*-switching, passive *Q*-switching is compact, and has simplicity in operation because it requires no electro-optic or acoustic-optic devices. Nowadays, the saturable absorbers for 1.3  $\mu\text{m}$  lasers comprise  $\text{V}^{3+}$ :YAG [1–3],  $\text{Co}^{2+}$ : $\text{MgAl}_2\text{O}_4$  [4],  $\text{Co}^{2+}$ :MAS [5], PbS-doped glasses [6], and semiconductor saturable absorber mirrors (SESAMs) [7–10]. The material for SESAMs at 1.3  $\mu\text{m}$  wavelength include InGaAs/GaAs quantum wells (QWs) [7], GaInNAs/GaAs QWs [8, 9], InAs/GaAs quantum dots (QDs) [10], and InGaAsP/InP bulk layers [11]. InGaAs QWs for 1.3  $\mu\text{m}$  SESAMs have the drawback of large insertion losses because the high indium concentration gives rise to significantly strained layers on the GaAs distributed Bragg reflectors (DBRs). Even though InAs QDs for 1.3  $\mu\text{m}$  SESAMs have lower nonsaturable losses, it is difficult to scale up the amount of the maximum reflectivity change between low and high intensities [10]. On the contrary, the lattice-matched InGaAsP-based SESAMs could offer saturable absorbers with larger modulation depths and longer recovery lifetimes for passive *Q*-switching operation at 1.3  $\mu\text{m}$ . However, the overall performance of the DBRs on InP substrates are hindered by the disadvantage

of a small contrast between refractive indices. Even though AlGaAsSb/InP has been demonstrated to be lattice-matched DBRs at 1.55  $\mu\text{m}$  [12], it is more difficult for the 1.3  $\mu\text{m}$  wavelength because the choice of DBR becomes tighter. Nevertheless, the DBRs are merely an optional structure for the cavity design of the passive *Q*-switched lasers. Without the use of DBRs, the semiconductor saturable absorber (SESA) has to be grown on a transparent substrate. The Fe-doped InP material is a particularly useful substrate to grow the SESA for passively *Q*-switched Nd-doped or Yb-doped solid-state lasers [13], since it is transparent at the lasing spectral region. More importantly, the double-pass configuration with an external output coupler is beneficial to the flexibility of the cavity design and the optimization of the output coupler.

Here we present an InGaAsP QW/barrier structure grown on an Fe-doped InP substrate to be a semiconductor saturable absorber (SESA) for a Nd:YVO<sub>4</sub> 1.34  $\mu\text{m}$  laser. The novelty of this work lies in the present semiconductor device serving simultaneously as a saturable absorber for 1.34  $\mu\text{m}$  lasers and a strong absorber for the suppression of the transition channel at 1.06  $\mu\text{m}$ . With an incident pump power of 1.8 W, an average output power of 160 mW with a peak power of 220 W at a pulse repetition rate of 38 kHz was obtained.

## 2 Experimental

This InGaAsP QW/barrier structure was monolithically grown on an Fe-doped InP substrate by metalorganic chemical-vapor deposition. The saturable-absorber region consists of fifteen InGaAsP QWs with the band-gap wavelength around 1.34  $\mu\text{m}$ , spaced at quarter-wavelength intervals by InGaAsP barrier layers with the band-gap wavelength around 1.06  $\mu\text{m}$ . In other words, the composition of the barrier layers was designed to have a strong absorbance at 1.06  $\mu\text{m}$ . With this SESA, the cavity mirrors require no special dichroic coatings to suppress the strongest transition channel at 1.06  $\mu\text{m}$ . The backside of the substrate was mechanically polished after growth. Both sides of the SESA were antireflection (AR) coated to reduce back reflections and couple-cavity effects. Figure 1 shows the transmittance spectrum at room temperature for the AR-coated InGaAsP/InP saturable absorber. The transmittance of the AR-coated Fe-doped InP substrate is also shown for comparison. It can be seen that the strong absorption of the barrier layers leads to

✉ Fax: +886-35-725230, E-mail: yfchen@cc.nctu.edu.tw

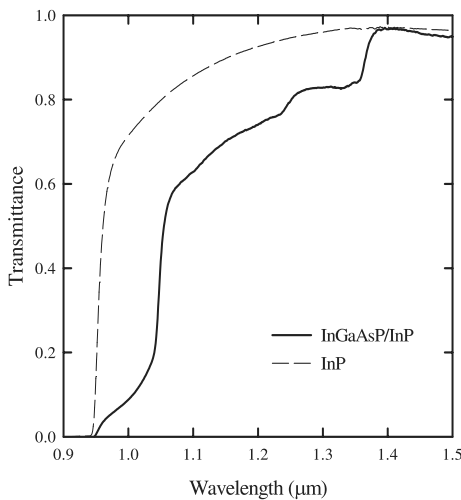


**FIGURE 1** Solid line: the transmittance spectrum at room temperature for the AR-coated InGaAsP/InP saturable absorber. Dashed line: the transmittance of the AR-coated Fe-doped InP substrate

a low transmittance near  $1.06 \mu\text{m}$ . The initial transmissions at  $1.06 \mu\text{m}$  and  $1.34 \mu\text{m}$  are 0.54 and 0.82, respectively. As a consequence, the gain suppression of  $1.06 \mu\text{m}$  is approximately 3 dB compared to that of  $1.34 \mu\text{m}$  for a double pass. On the other hand, an abrupt change in the transmittance near  $1.36 \mu\text{m}$  comes from the absorption of the InGaAsP QWs. The modulation depth of the SESA device is experimentally estimated to be approximately 10% in a single pass, so in total 20% for a cavity roundtrip. From the numerical simulations of the SESA design, the saturation fluence is estimated to be in the range of  $10 \mu\text{J}/\text{cm}^2$ . The relaxation time and optical damage threshold of the SESA are approximately  $10 \sim 20 \text{ ns}$  and  $200 \sim 300 \text{ MW}/\text{cm}^2$ , respectively.

Figure 2 depicts the experimental configuration for the passively  $Q$ -switched  $1.34 \mu\text{m}$  Nd:YVO<sub>4</sub> laser by use of InGaAsP/InP QWs as a saturable absorber. The active medium was a 0.5 at. % Nd<sup>3+</sup>, 6 mm long Nd:YVO<sub>4</sub> crystal. Both sides of the laser crystal were coated for antireflection at  $1.34 \mu\text{m}$  ( $R < 0.2\%$ ). The pump source was a 2.0 W 808 nm fiber-coupled laser diode with a core diameter of  $200 \mu\text{m}$  and

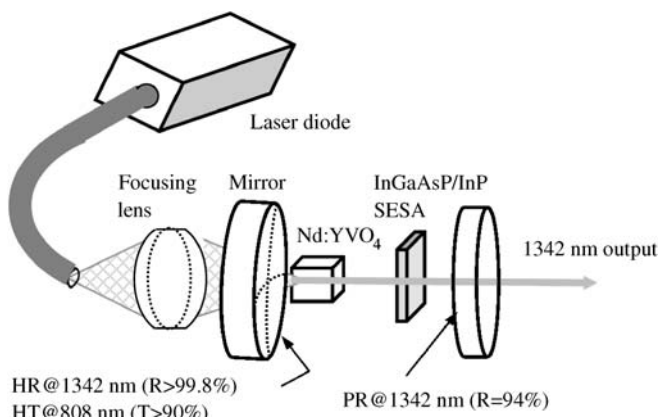


**FIGURE 2** Experimental configuration for the passively  $Q$ -switched  $1.34 \mu\text{m}$  Nd:YVO<sub>4</sub> laser by use of InGaAsP/InP QWs as a saturable absorber

a numerical aperture of 0.16. A focusing lens with a 16.5 mm focal length and 90% coupling efficiency was used to re-image the pump beam into the laser crystal. The pump spot radius was around  $100 \mu\text{m}$ . The input mirror was a 500 mm radius-of-curvature concave mirror with antireflection coating at the diode wavelength on the entrance face ( $R < 0.2\%$ ), high-reflection coating at the lasing wavelength ( $R > 99.8\%$ ) and a high-transmission coating at the diode wavelength on the other surface ( $T > 90\%$ ). Note that the laser crystal was placed near the input mirror ( $< 1 \text{ mm}$ ) for the spatial overlap of the transverse mode structure and radial pump power distribution. The reflectivity of the output coupler is 94% at  $1342 \text{ nm}$ . The overall Nd:YVO<sub>4</sub> laser cavity length was approximately 20 mm. The cavity losses introduced by the pump mirror and output coupler are approximately 0.48 and 0.065 for wavelengths at  $1.06$  and  $1.34 \mu\text{m}$ . The total nonsaturable loss introduced by the SESA is approximately 0.05. The nonsaturable loss of the SESA mainly comes from electron overflow. The nonsaturable loss may be reduced by the QW materials with relatively large conduction band offsets. Without the SESA in the cavity, cw operation at  $1.34 \mu\text{m}$  could be achieved with the cavity losses introduced by the resonator mirrors. However, the gain suppression at  $1.06 \mu\text{m}$  needed to be larger for the  $Q$ -switching operation at  $1.34 \mu\text{m}$ . In the present setup, the extra gain suppression at  $1.06 \mu\text{m}$  was introduced by the SESA.

### 3 Results and discussion

Figure 3 shows the average output powers at  $1342 \text{ nm}$  with respect to the incident pump power in cw and passively  $Q$ -switching operations. Without the SESA in the cavity, the cw laser at  $1342 \text{ nm}$  had a slope efficiency of 37% and an output power of 580 mW at an incident pump power of 1.8 W. In the passively  $Q$ -switching regime an average output power of 160 mW was obtained at an incident pump power of 1.8 W. The  $Q$ -switching efficiency (ratio of the  $Q$ -switched output power to the cw power at the maximum pump power) was found to be 27.6%. This  $Q$ -switching efficiency is considerably higher than that obtained with an InGaAsP SESAM [4]

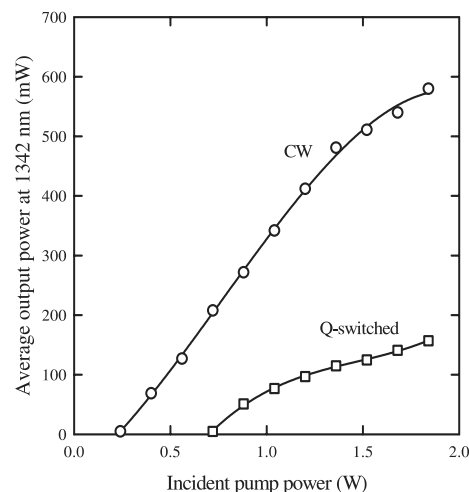


**FIGURE 3** Average output powers at  $1.34 \mu\text{m}$  with respect to the incident pump power in cw and passively  $Q$ -switching operations

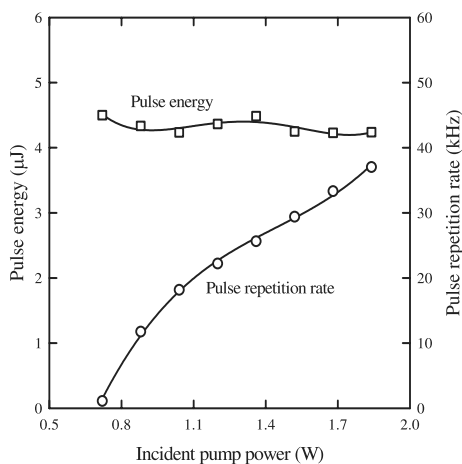


**FIGURE 4** Experimental results for the pulse repetition rate and the pulse width versus incident pump power

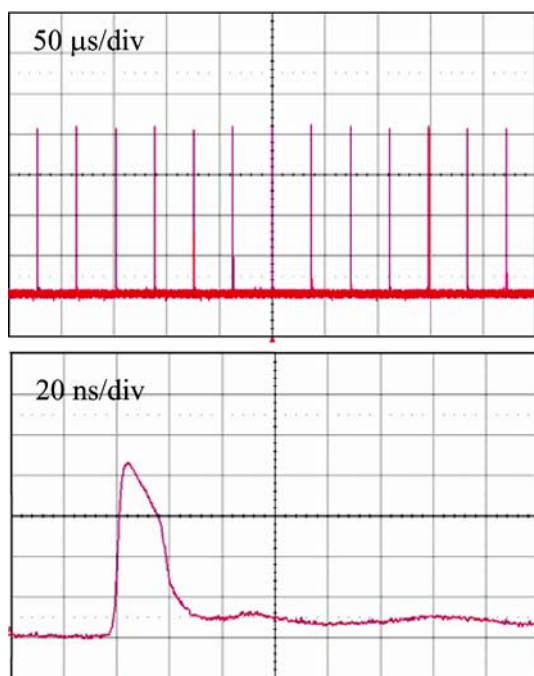


**FIGURE 5** (a) Typical oscilloscope trace of a train of output pulses and (b) expanded shape of a single pulse

and is close to the results obtained with  $\text{V}^{3+}:\text{YAG}$  [1–3] and  $\text{Co}^{2+}:\text{MAS}$  [5] saturable absorbers.

The pulse temporal behavior was recorded by a LeCroy digital oscilloscope (Wavepro 7100, 10 G – samples/sec, 1 GHz bandwidth) with a fast p-i-n photodiode. Figure 4 shows the pulse repetition rate and the pulse energy versus the incident pump power. The pulse repetition rate increases monotonically with the pump power up to 38 kHz.

On the other hand, the pulse energy, like typical passively  $Q$ -switched lasers, is insensitive to the pump power. A typical oscilloscope trace of a train of output pulses and an expanded shape of a single pulse are shown in Fig. 5. Under the optimum alignment condition, the pulse-to-pulse amplitude fluctuation was found to be within  $\pm 5\%$ . The pulse width was measured to be 19 ns. As a consequence, the peak power was found to be higher than 220 W. It is worthwhile mentioning that although the  $\text{Nd}:\text{YVO}_4$  crystal is an efficient Raman gain medium, the present intracavity peak power is not high enough to reach the Raman self-conversion.

The InGaAsP QW/barrier structure grown on a Fe-doped substrate was used as a saturable absorber for the  $Q$ -switching of a diode-pumped  $\text{Nd}:\text{YVO}_4$  laser operating at 1342 nm. An average output power of 160 mW was obtained at an incident pump power of 1.8 W. Stable  $Q$ -switched pulses of 19 ns duration with a repetition rate of 38 kHz were generated. The present result indicates the possibility of using InGaAsP QW/barrier structure to generate a  $Q$ -switched 1.3  $\mu\text{m}$  laser with peak power greater than 1 kW. Attempts to use InGaAsP-based SESA to scale up Nd-doped 1.3  $\mu\text{m}$  lasers are under way.

**ACKNOWLEDGEMENTS** The authors gratefully acknowledge various InGaAsP/InP QW structures from TrueLight Corporation. The authors also thank the National Science Council for their financial support of this research under contract No. NSC-93-2112-M-009-034.

## REFERENCES

- 1 A.M. Malyarevich, I.A. Denisov, K.V. Yumashev, V.P. Mikhailov, R.S. Conroy, B.D. Sinclair, *Appl. Phys. B* **67**, 555 (1998)
- 2 A.S. Grabtchikov, A.N. Kuzmin, V.A. Lisinetskii, V.A. Orlovich, A.A. Demidovich, K.V. Yumashev, N.V. Kuleshov, H.J. Eichler, M.V. Danailov, *Opt. Mater.* **16**, 349 (2001)
- 3 A. Agnesi, A. Guandalini, G. Reali, J.K. Jabczynski, K. Kocpzyński, Z. Mierczyk, *Opt. Commun.* **194**, 429 (2001)
- 4 K.V. Yumashev, I.A. Denisov, N.N. Posnov, P.V. Prokoshin, V.P. Mikhailov, *Appl. Phys. B* **70**, 179 (2000)
- 5 Y.V. Volk, I.A. Denisov, A.M. Malyarevich, K.V. Yumashev, O.S. Dymshits, A.V. Shashkin, A.A. Zhilin, U. Kang, K.H. Lee, *Appl. Opt.* **43**, 682 (2004)
- 6 V.G. Savitski, N.N. Posnov, P.V. Prokoshin, A.M. Malyarevich, K.V. Yumashev, M.I. Demchuk, A.A. Lipovski, *Appl. Phys. B* **75**, 841 (2002)
- 7 R. Fluck, Z. Zhang, U. Keller, K.J. Weingarten, M. Moser, *Opt. Lett.* **21**, 1378 (1996)
- 8 H.D. Sun, G.J. Valentine, R. Macaluso, S. Calvez, D. Burns, M.D. Dawson, T. Jouhti, M. Pessa, *Opt. Lett.* **27**, 2124 (2002)
- 9 V. Liverini, S. Schön, R. Grange, M. Haiml, S.C. Zeller, U. Keller, *Appl. Phys. Lett.* **84**, 4002 (2004)
- 10 H.C. Lai, A. Li, K.W. Su, M.L. Ku, Y.F. Chen, K.F. Huang, *Opt. Lett.* **30**, 480 (2005)
- 11 R. Fluck, B. Braun, E. Gini, H. Melchior, U. Keller, *Opt. Lett.* **22**, 991 (1997)
- 12 O. Ostinelli, W. Bächtold, M. Haiml, R. Grange, U. Keller, M. Ebnöther, E. Gini, G. Almuneau, *J. Cryst. Growth* **286**, 247 (2006)
- 13 Y. Tsou, E. Garmire, W. Chen, M. Birnbaum, R. Asthana, *Opt. Lett.* **18**, 1514 (1993)